

ELECTRONIC SUPPLEMENTARY INFORMATION

Reactivity of mononuclear Pd(II) and Pt(II) complexes containing the primary phosphane (ferrocenylmethyl)phosphane towards metal chlorides and PPh₃.

Maria Michela Dell'Anna^a, Piero Mastrorilli^{a*}, Cosimo Francesco Nobile^a, Beatrice Calmuschi-Cula^b, Ulli Englert^b, Maurizio Peruzzini^c

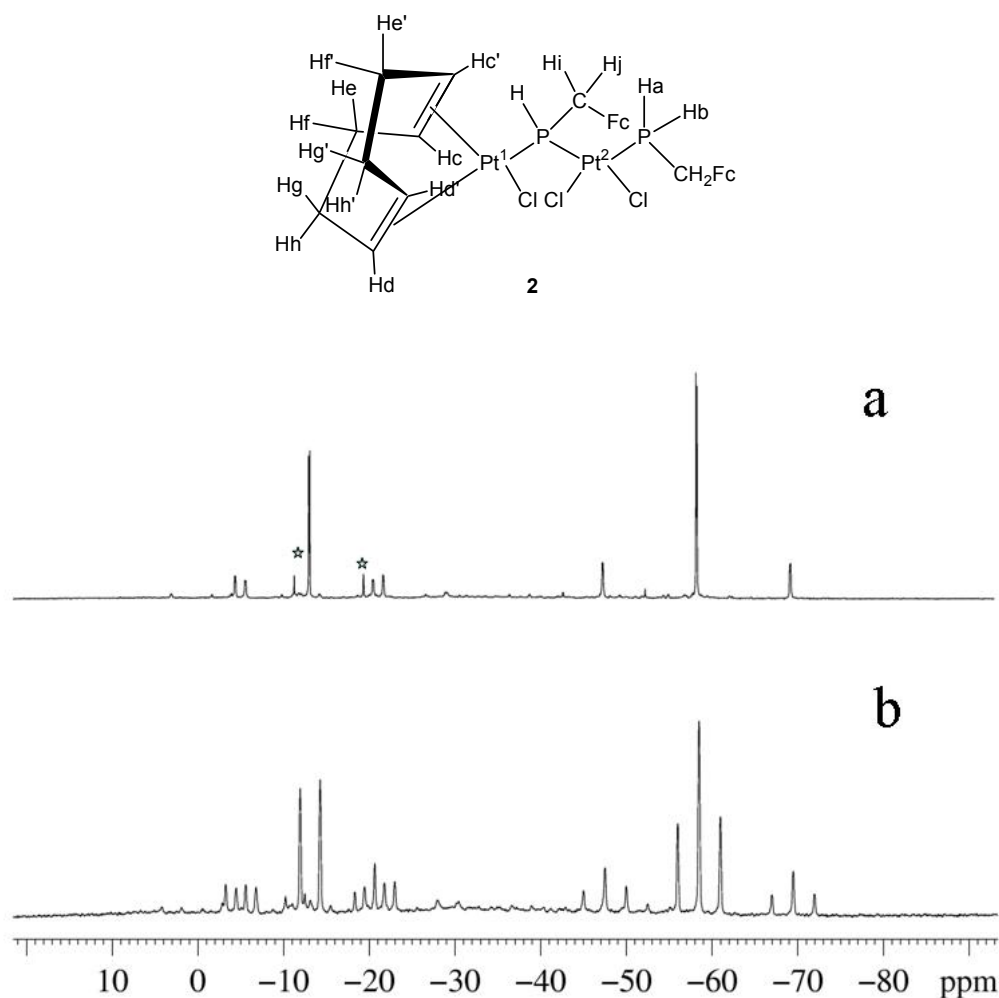


Figure S1: (a) ³¹P{¹H} and (b) ³¹P NMR spectra of **2** (CD₂Cl₂, 273 K, 162 MHz). The starred peaks are due to impurities.

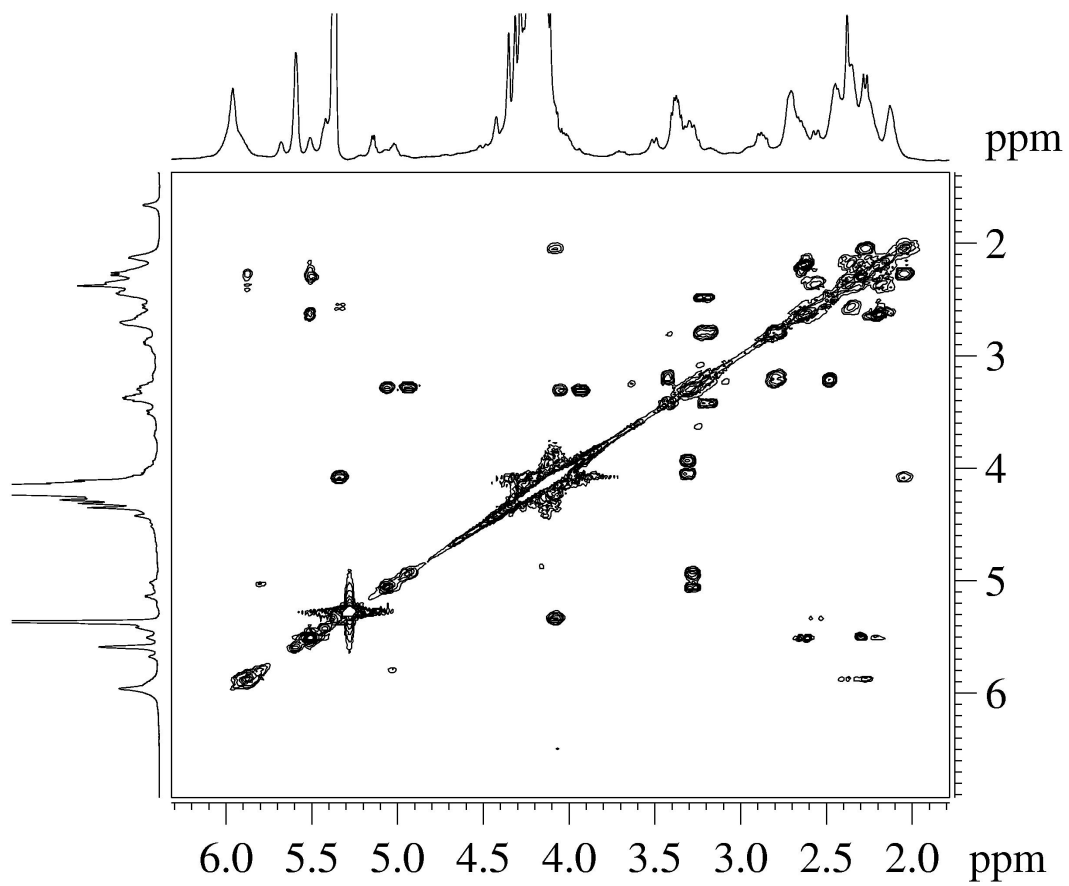


Figure S2: ^1H -COSY spectrum of **2** (CD_2Cl_2 , 273 K, 400 MHz).

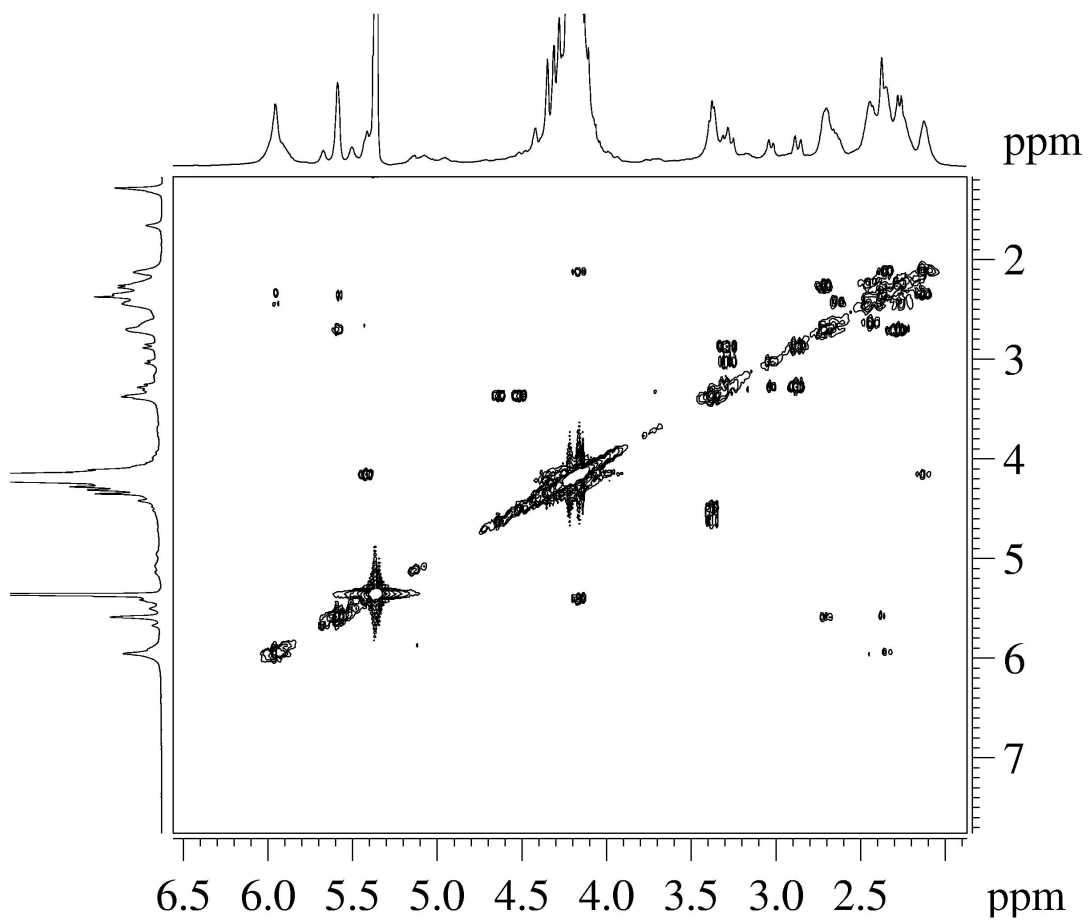


Figure S3: $^1\text{H}\{^{31}\text{P}\}$ -COSY spectrum of **2** (CD_2Cl_2 , 273 K, 400 MHz).

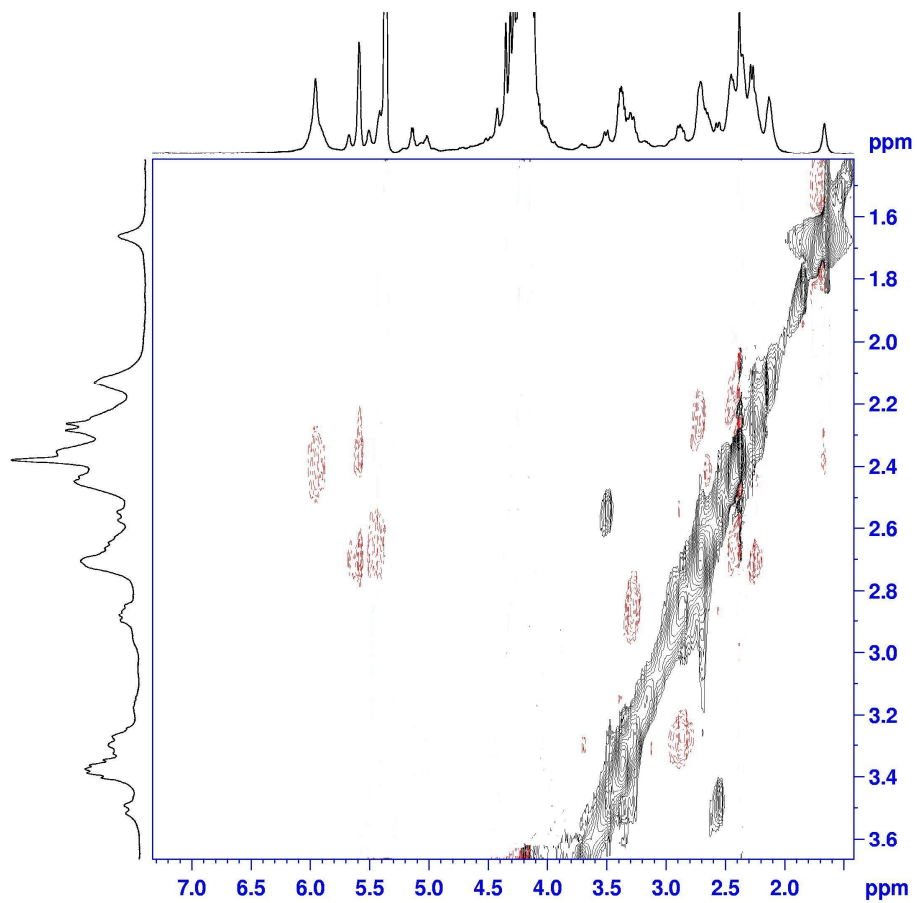


Figure S4: portion of the ^1H -NOESY spectrum of **2** (CD_2Cl_2 , 273 K, 400 MHz): the red cross peaks indicate *noesy* interaction.

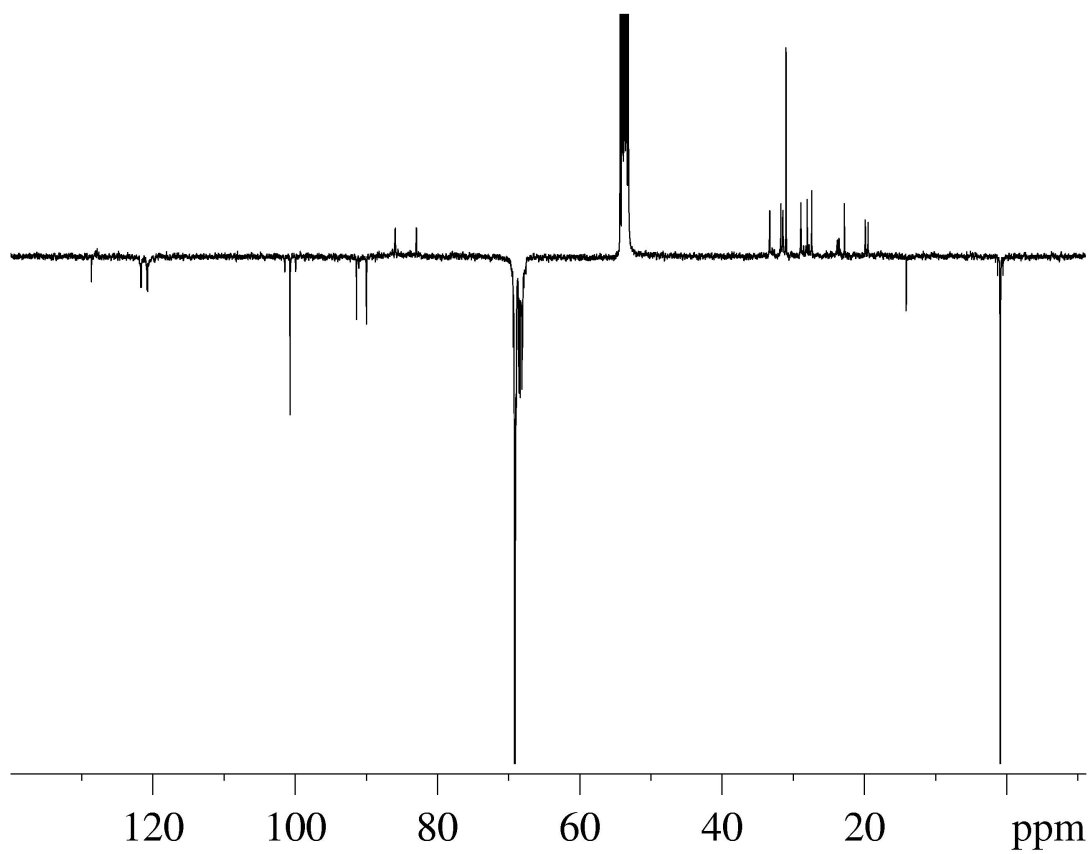


Figure S5: $^{13}\text{C}\{^1\text{H}\}$ APT NMR spectrum of **2** (CD_2Cl_2 , 273 K, 100 MHz, *C* and CH_2 point upward, *CH* and CH_3 point downward).

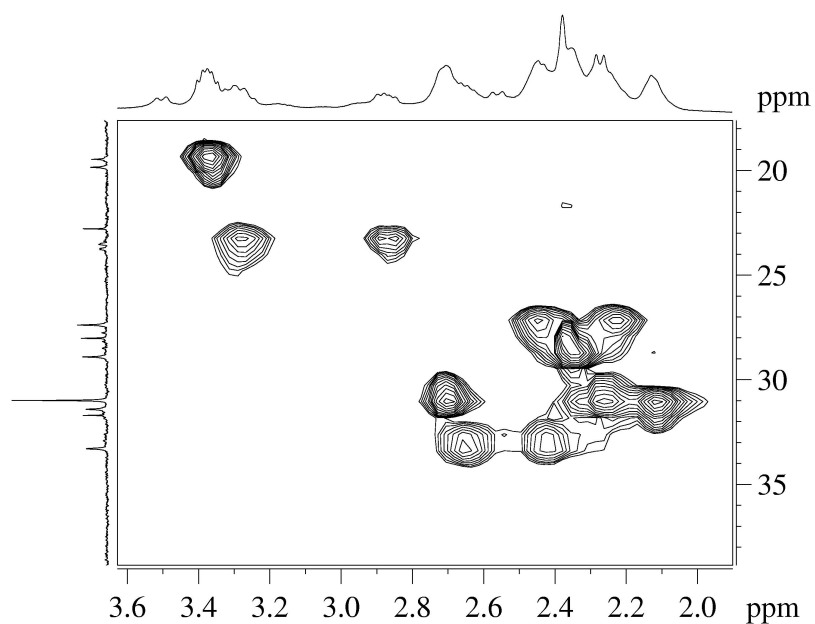


Figure S6: portion of the ^1H - ^{13}C HMQC spectrum of complex **2** in the methylenic region (CD_2Cl_2 , 273 K).

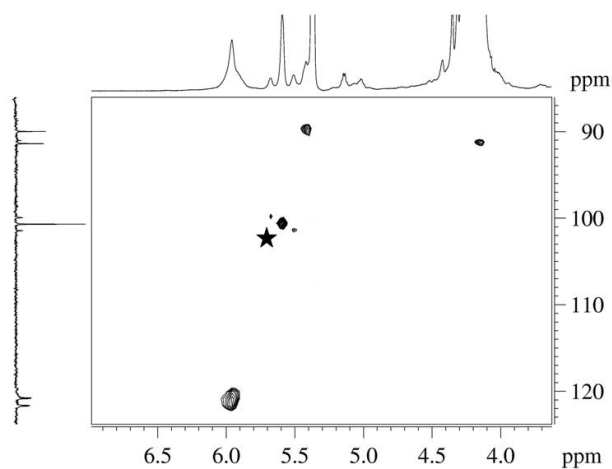


Figure S7: Portion of the ^1H - ^{13}C HMQC spectrum of **2** in the vinylic region (CD_2Cl_2 , 273 K). In the $^{13}\text{C}\{^1\text{H}\}$ APT NMR spectrum of F1 the signals of primary and tertiary carbons point downward. The starred cross peak is due to the $[\text{Pt}(\text{cod})\text{Cl}_2]$ impurity.

$^{13}\text{C}\{^1\text{H}\}$ -APT and ^1H - ^{13}C HMQC spectra of **2** (Figure S5-7) show the magnetic inequivalence of the four vinylic carbon nuclei.

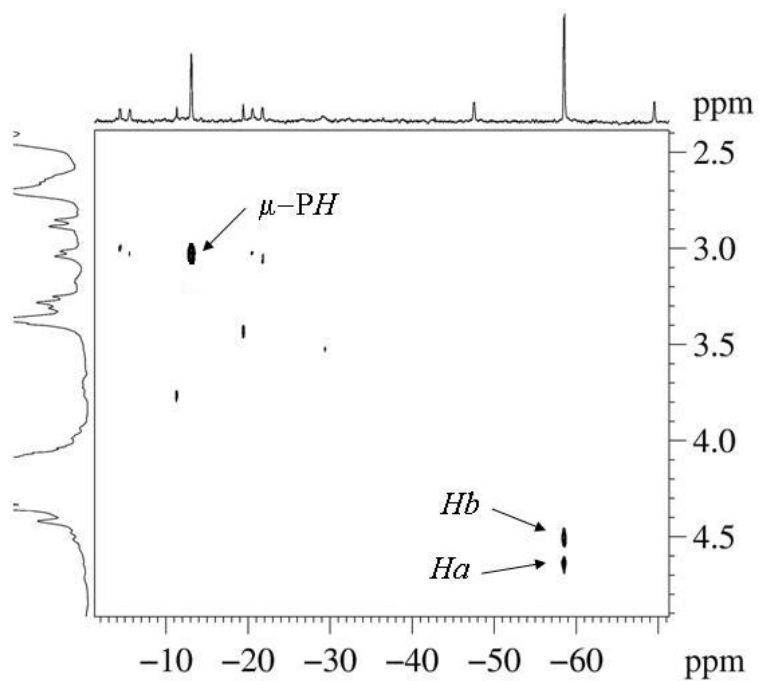


Figure S8: ^{31}P - ^1H HETCOR spectrum of **2** (CD_2Cl_2 , 273 K). The projection on F1 is the $^1\text{H}\{^{31}\text{P}\}$ NMR spectrum.

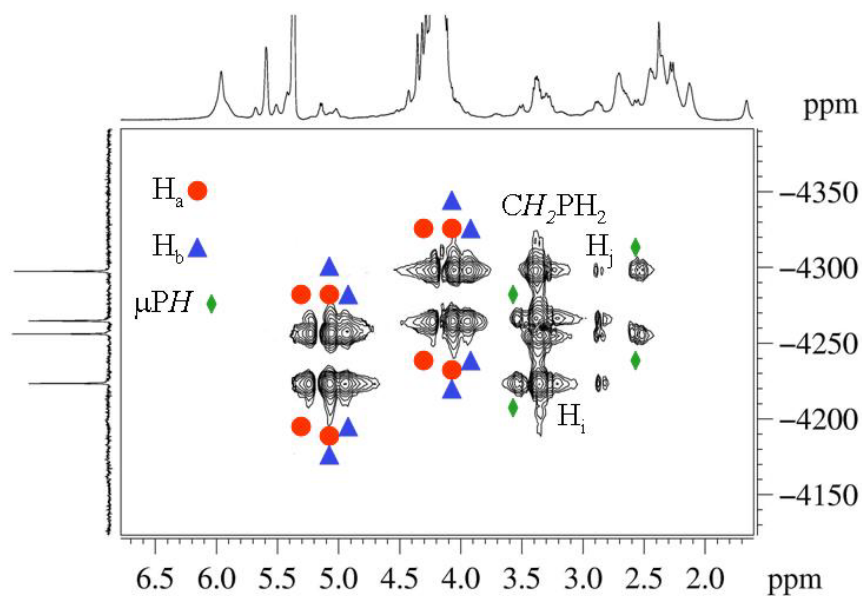


Figure S9: Portion of the ^1H - ^{195}Pt HMQC spectrum of **2** (CD_2Cl_2 , 273 K, Pt^2 region).

The ^1H - ^{195}Pt HMQC spectrum of **2** in Figure S9 shows that the four different vinylic protons of the coordinated diene couple only with Pt^1 (H_d and H_d' , $\delta_{\text{H}_d'} = \delta_{\text{H}_d} = 5.86$, $^2J_{\text{H}_d-\text{Pt}1} = ^2J_{\text{H}_d'-\text{Pt}1} = 40$ Hz; H_c' , $\delta_{\text{H}_c'} = 5.33$, $^2J_{\text{H}_c'-\text{Pt}1} = 72$ Hz; H_c , $\delta_{\text{H}_c} = 4.06$, $^2J_{\text{H}_c-\text{Pt}1} = 77$ Hz). The chemical shifts of the diastereotopic vinylic protons *cis* to the phosphido bridging ligand (H_c and H_c') are significantly different; on the contrary, the chemical shifts of the diastereotopic vinylic protons *trans* to the phosphido bridging ligand (H_d and H_d') are coincident.

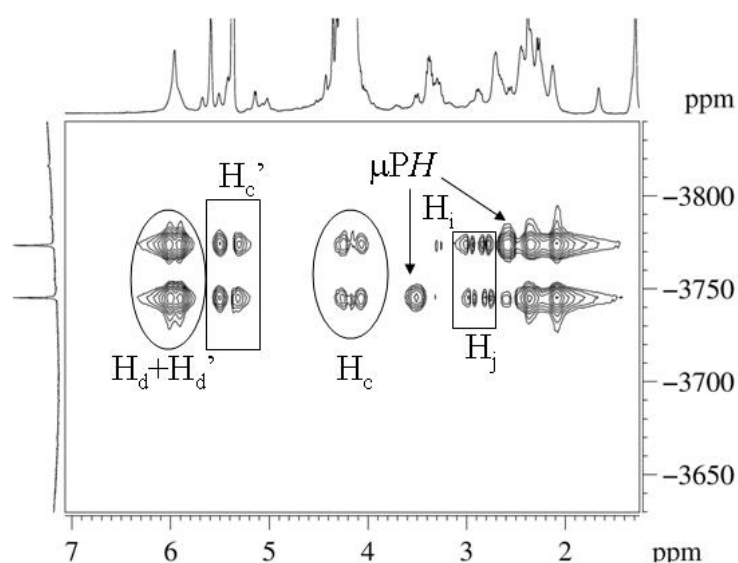


Figure S10: Portion of the ^1H - ^{195}Pt HMQC spectrum of **2** (CD_2Cl_2 , 273 K, Pt^1 region).

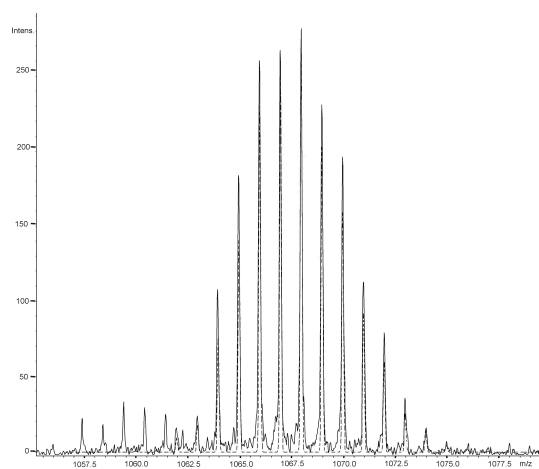


Figure S11: Experimental (solid line) and simulated (dashed line) HRMS(+) spectrum of **2** (exact mass = 1065.9425 da) in THF diluted with CH₃CN. The error between simulated and observed isotopic patterns is -0.9 ppm.

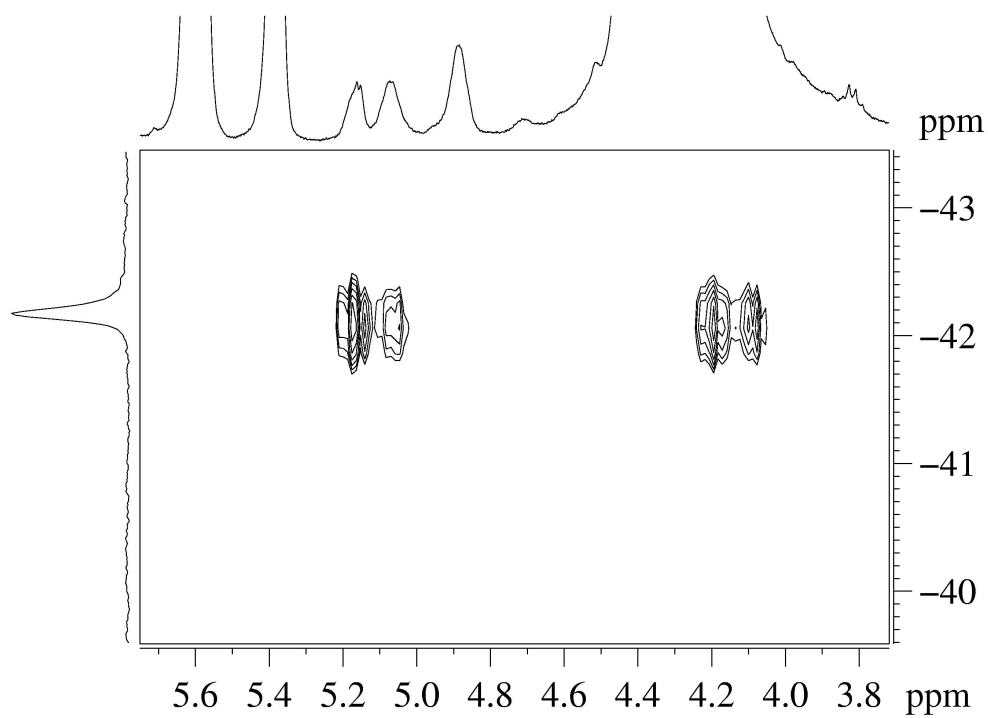
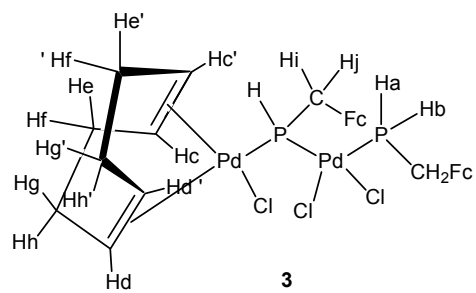


Figure S12: portion of the ^1H - ^{31}P HMQC spectrum of **3** (CD_2Cl_2 , 265 K) in the terminal phosphane region.

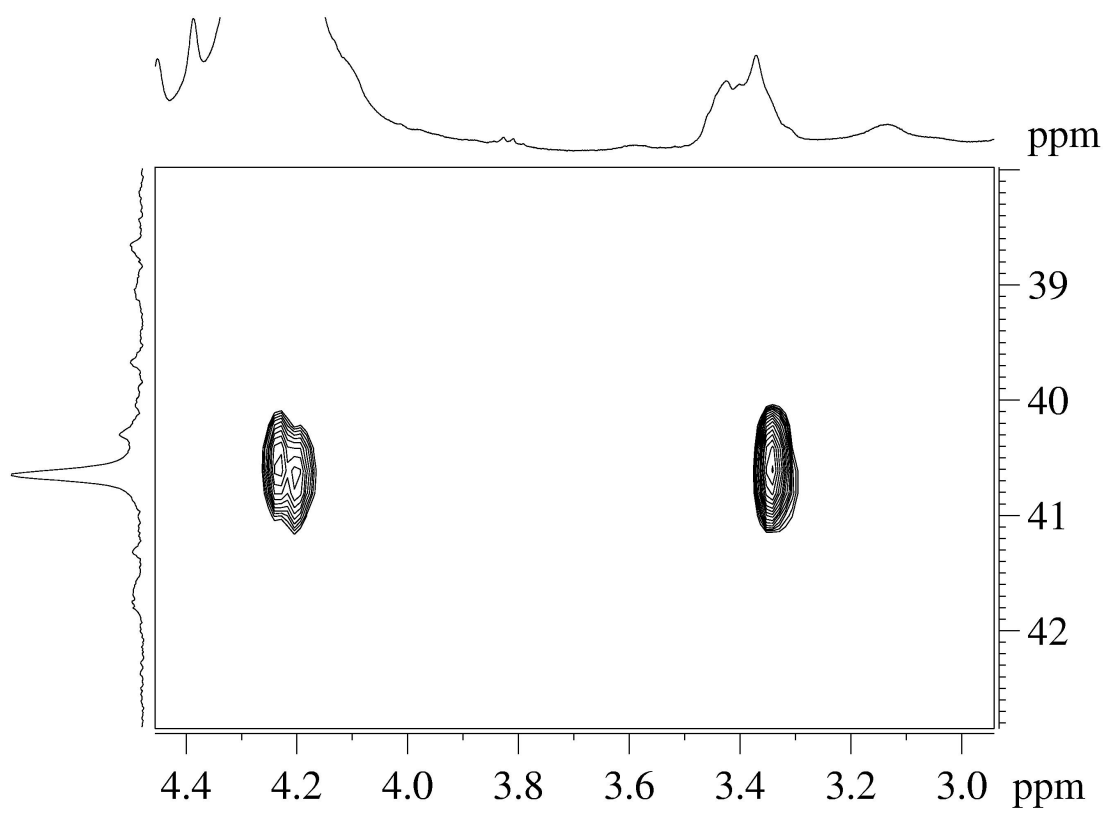


Figure S13: portion of the ^1H - ^{31}P HMQC spectrum of **3** (CD_2Cl_2 , 265 K) in the phosphido-bridged region.

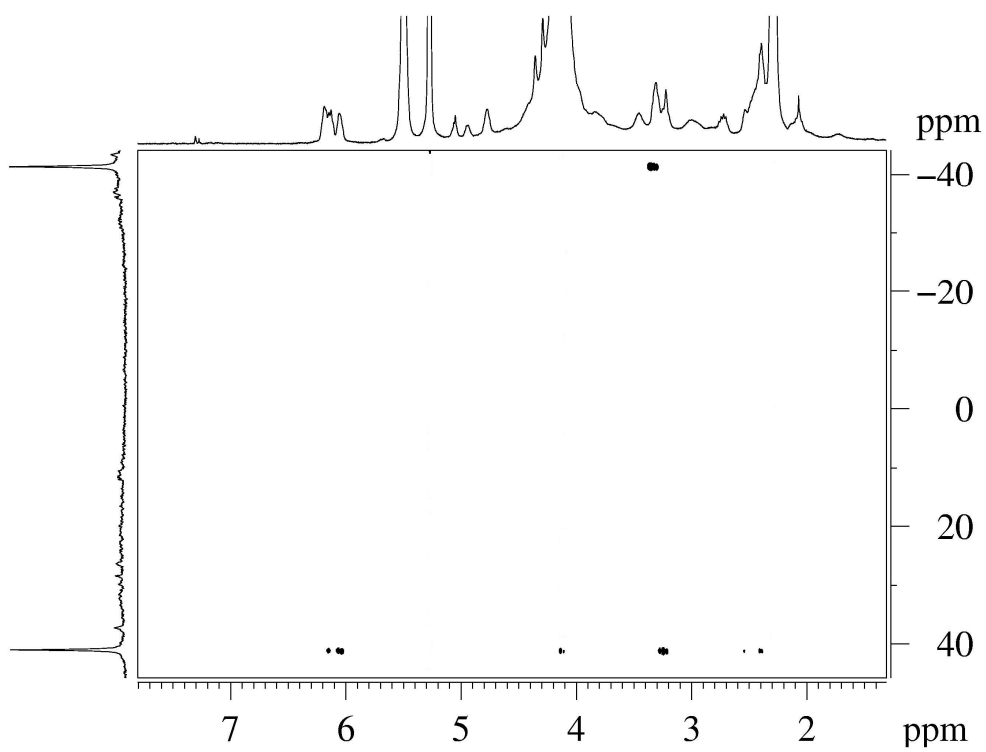


Figure S14: ^1H - ^{31}P HMBC spectrum of **3** (CD_2Cl_2 , 265 K).

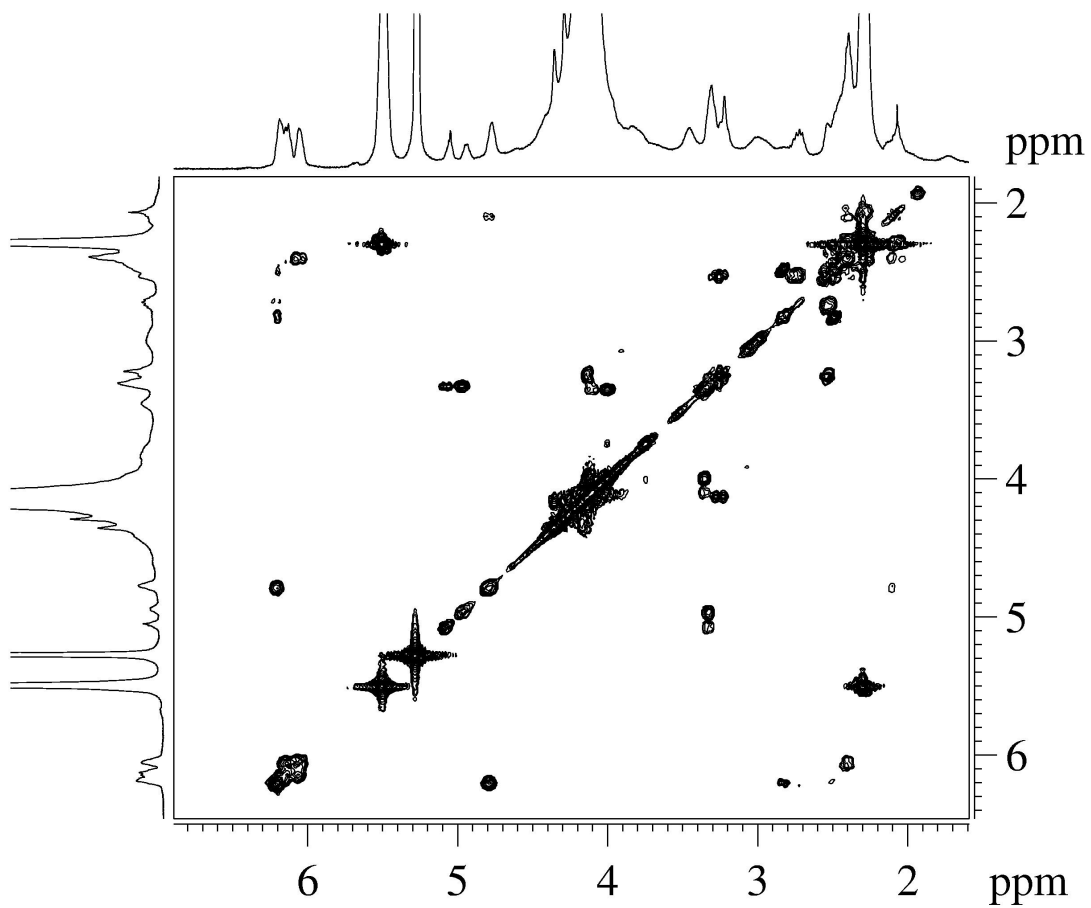


Figure S15: ^1H -COSY spectrum of **3** (CD_2Cl_2 , 265 K, 400 MHz).

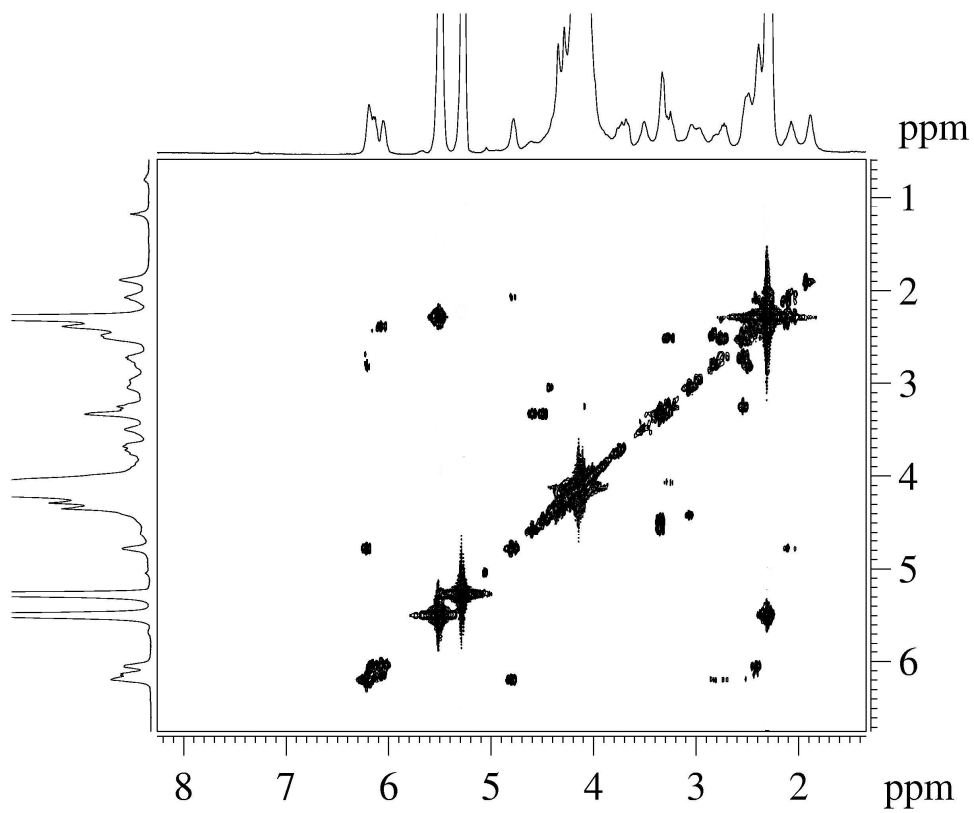


Figure S16: $^1\text{H}\{^{31}\text{P}\}$ -COSY spectrum of **3** (CD_2Cl_2 , 265 K, 400 MHz).

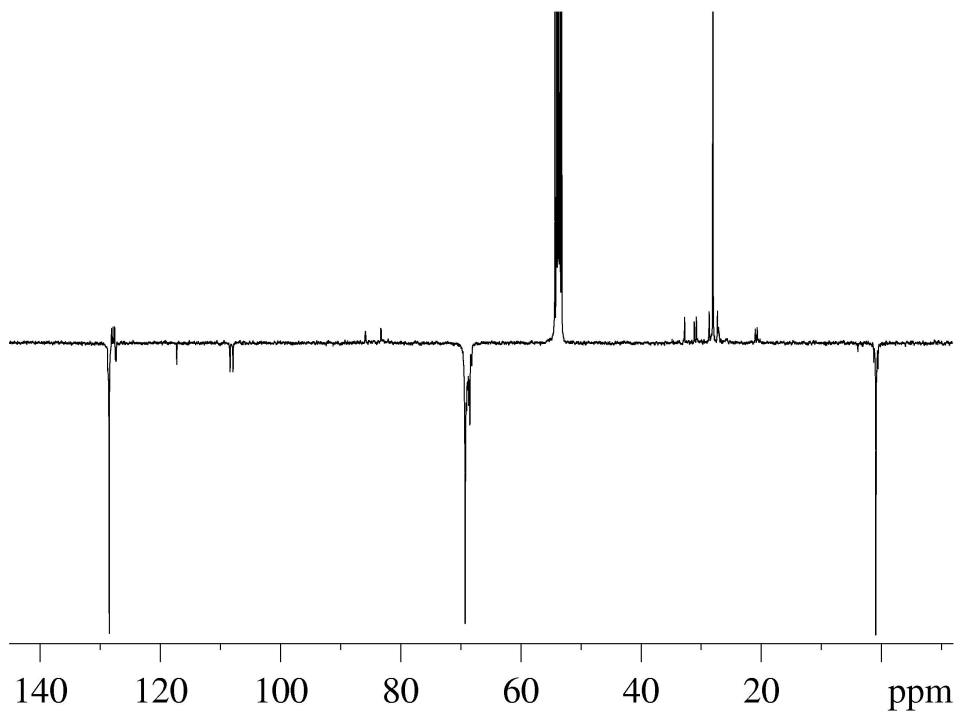


Figure S17: $^{13}\text{C}\{^1\text{H}\}$ APT NMR spectrum of **3** (CD_2Cl_2 , 265 K, 100 MHz, *C* and CH_2 point upward, CH and CH_3 point downward).

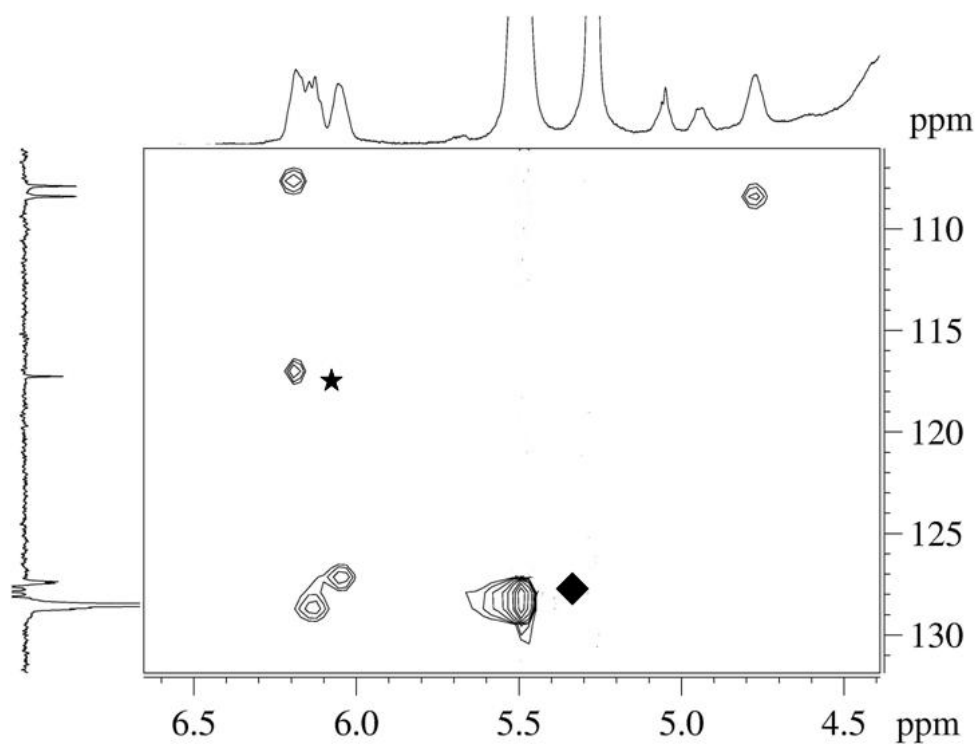


Figure S18: Portion of the ^1H - ^{13}C HMQC spectrum of complex **3** in the vinylic region (CD_2Cl_2 , 265 K). In the reported $^{13}\text{C}\{^1\text{H}\}$ APT NMR spectrum (F1) the signals of primary and tertiary carbons point downward. The cross-peaks marked with the star and with the rhomb are due to the vinylic protons of $[\text{Pd}(\text{cod})\text{Cl}_2]$ and of free COD impurities, respectively.

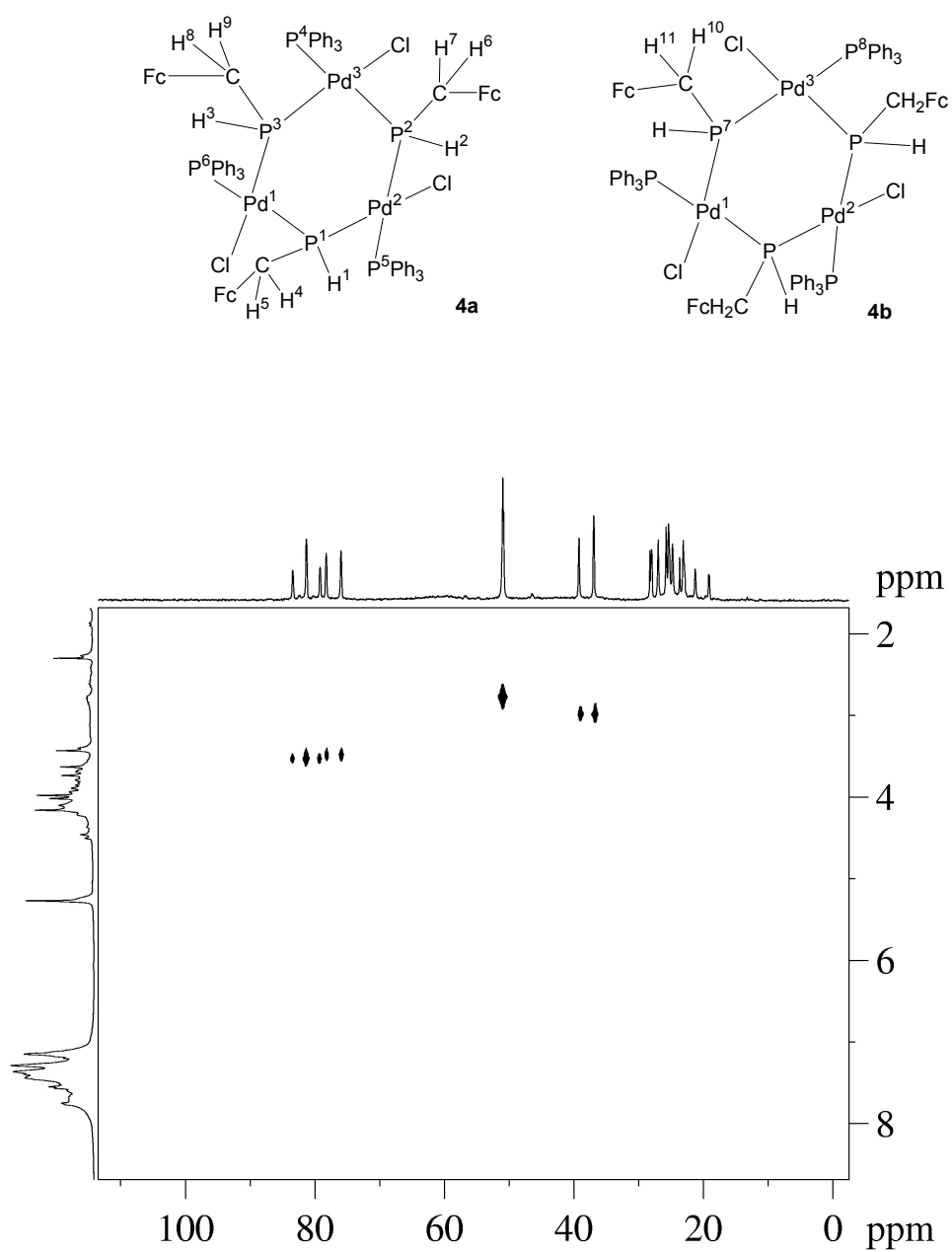


Figure S19: ^{31}P - ^1H HETCOR spectrum of **4a** and **4b** (CD_2Cl_2 , 295 K). The projection on F1 is the

$^1\text{H}\{^{31}\text{P}\}$ NMR spectrum.

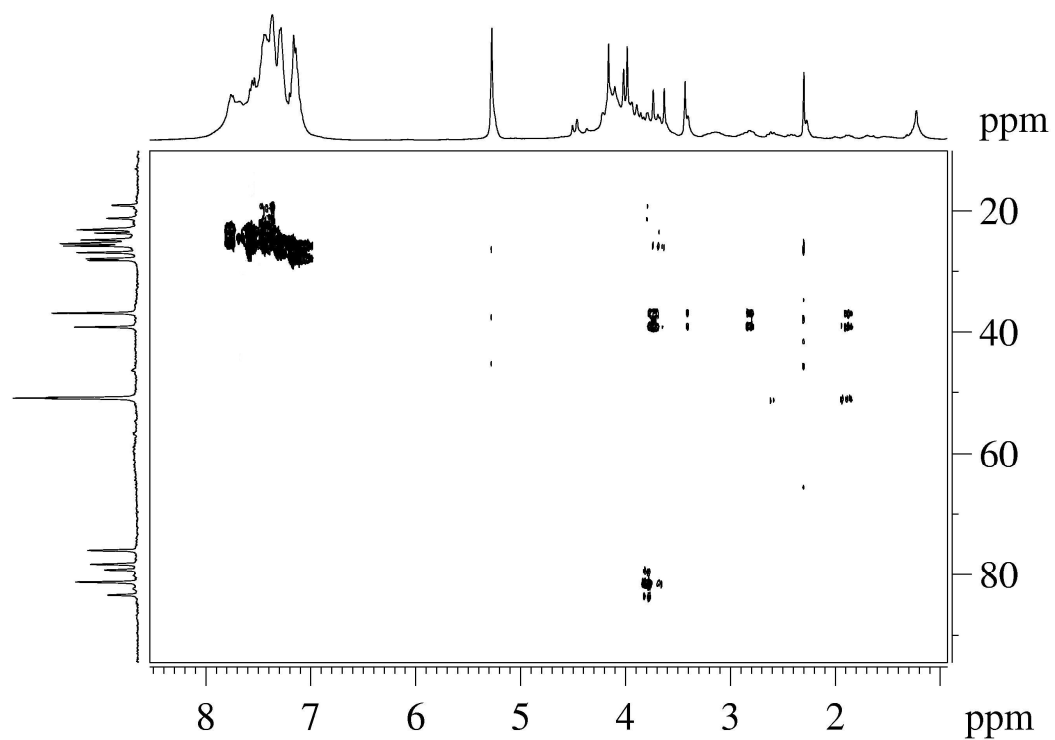


Figure S20: ^1H - ^{31}P HMBC spectrum of **4a** and **4b** (CD_2Cl_2 , 295 K)

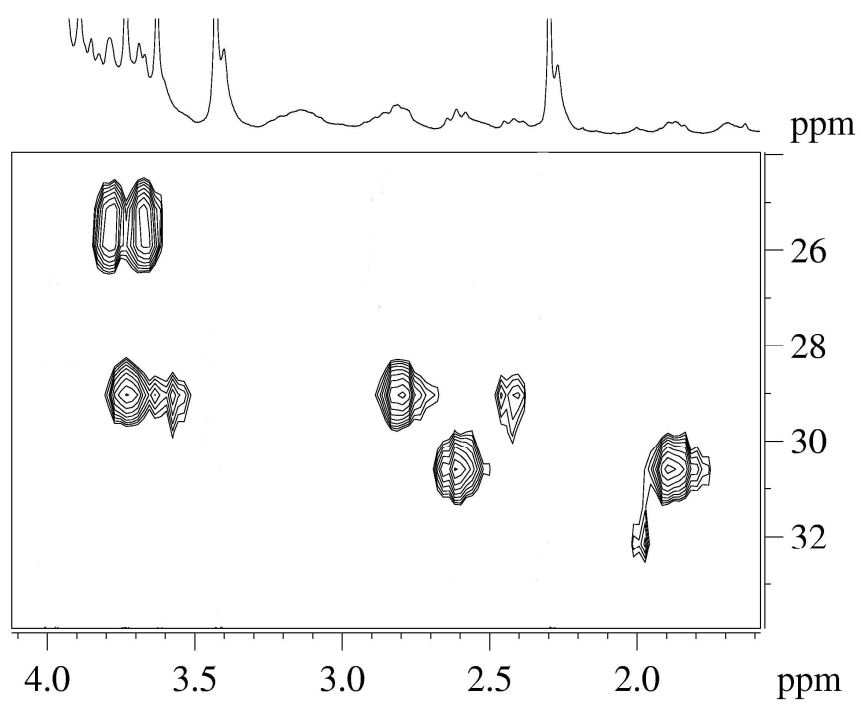


Figure S21: Methylenic region of the ^1H - ^{13}C -HMQC spectrum of **4a** and **4b** (CD_2Cl_2 , 295 K)

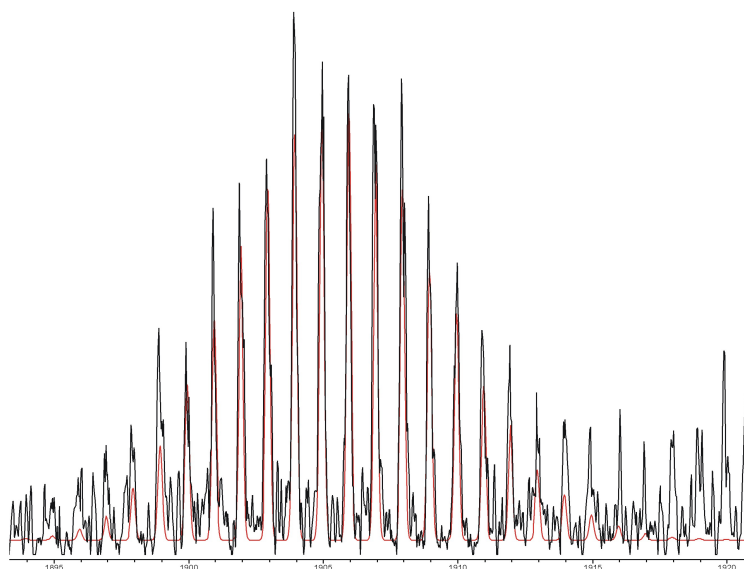


Figure S22: Experimental (black line) and simulated (red line) HRMS(+) spectrum of **4a** and **4b** (exact mass = 1901.8977 da) in THF diluted with CH₃CN. The error between simulated and observed isotopic patterns is 6.8 ppm.

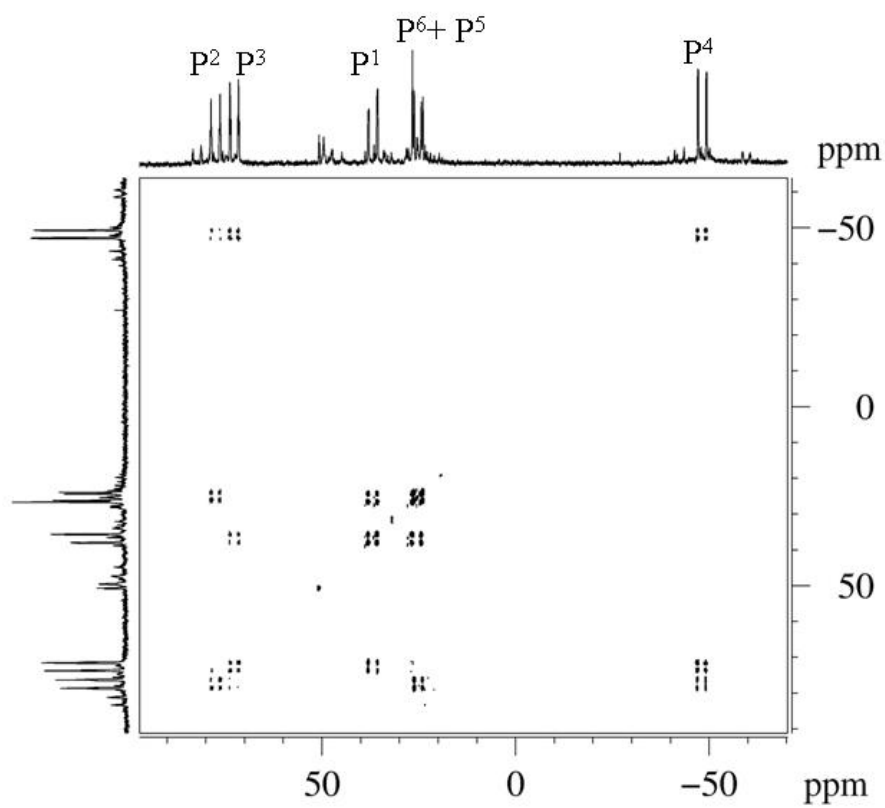
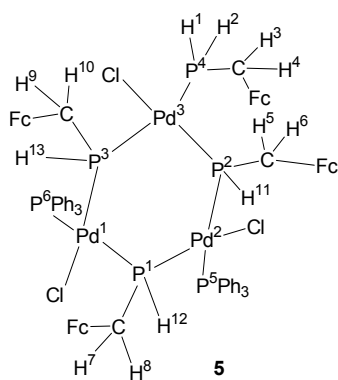


Figure S23: $^{31}\text{P}\{^1\text{H}\}$ -COSY spectrum (CD_2Cl_2 , 295 K) of **5**.

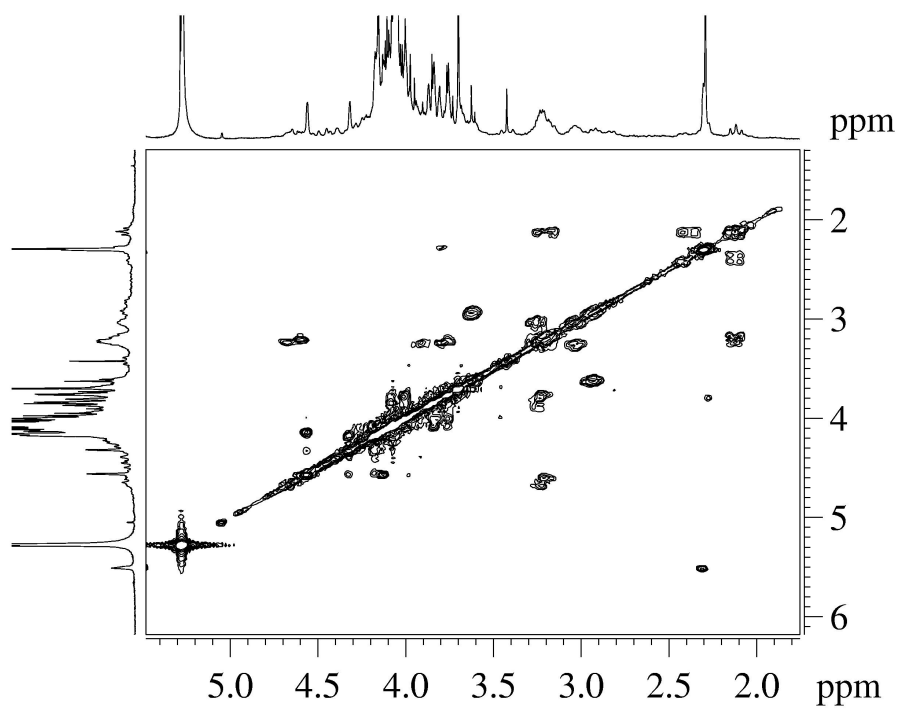


Figure S24: Portion of ^1H -COSY spectrum of **5** (CD_2Cl_2 , 295 K).

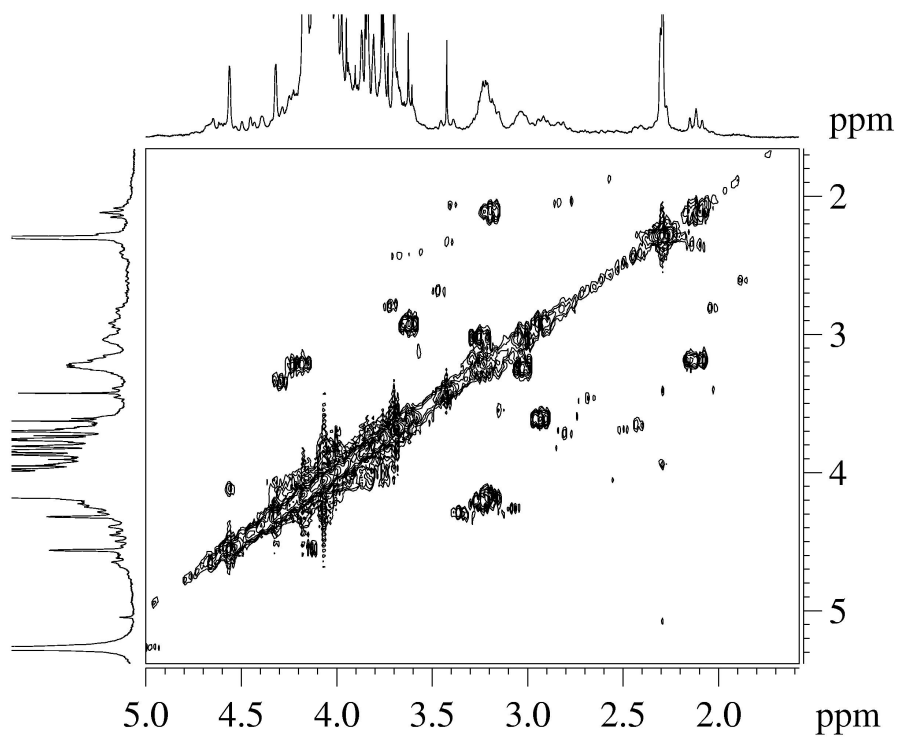


Figure S25: Portion of $^1\text{H}\{^{31}\text{P}\}$ -COSY spectrum of **5** (CD_2Cl_2 , 295 K).

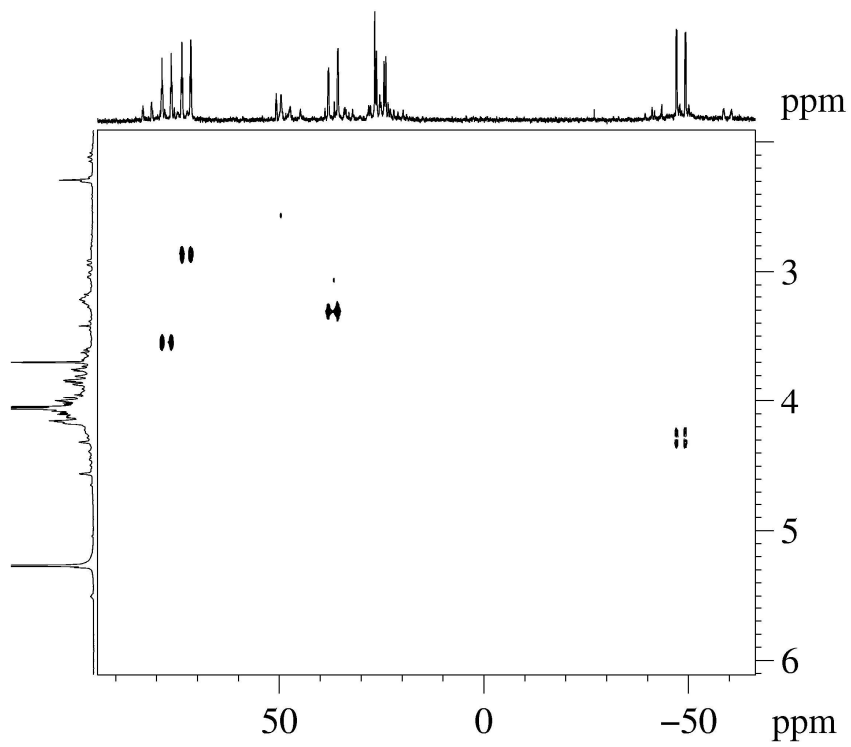


Figure S26: ^{31}P - ^1H HETCOR spectrum of **5** (CD_2Cl_2 , 295 K). The projection in F1 is the $^1\text{H}\{^{31}\text{P}\}$ NMR spectrum.

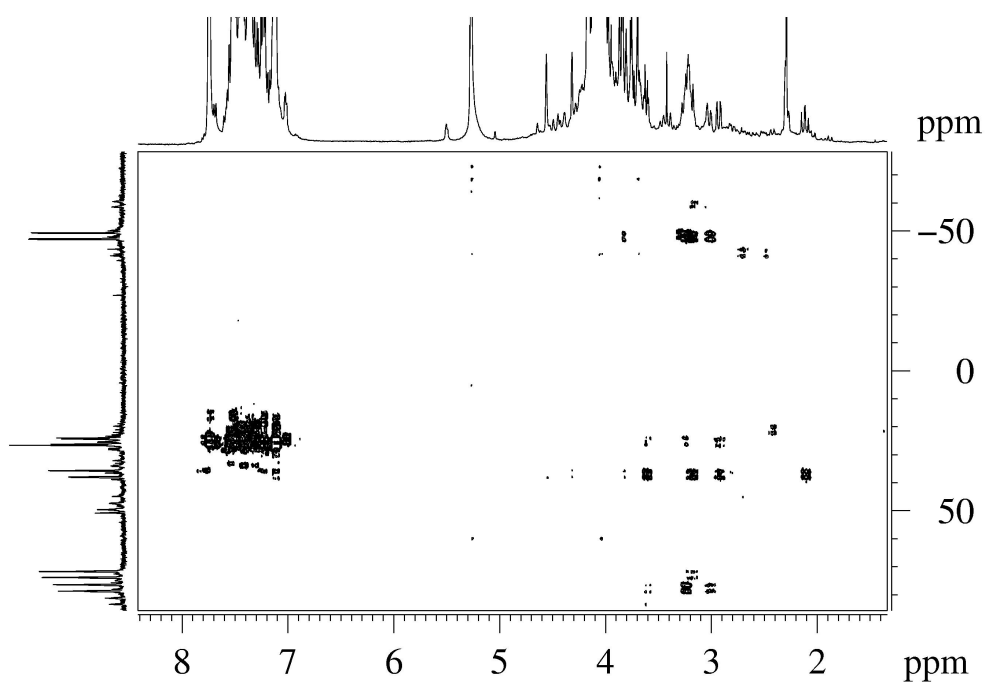


Figure S27: ^1H - ^{31}P HMBC spectrum of **5** (CD_2Cl_2 , 295 K)

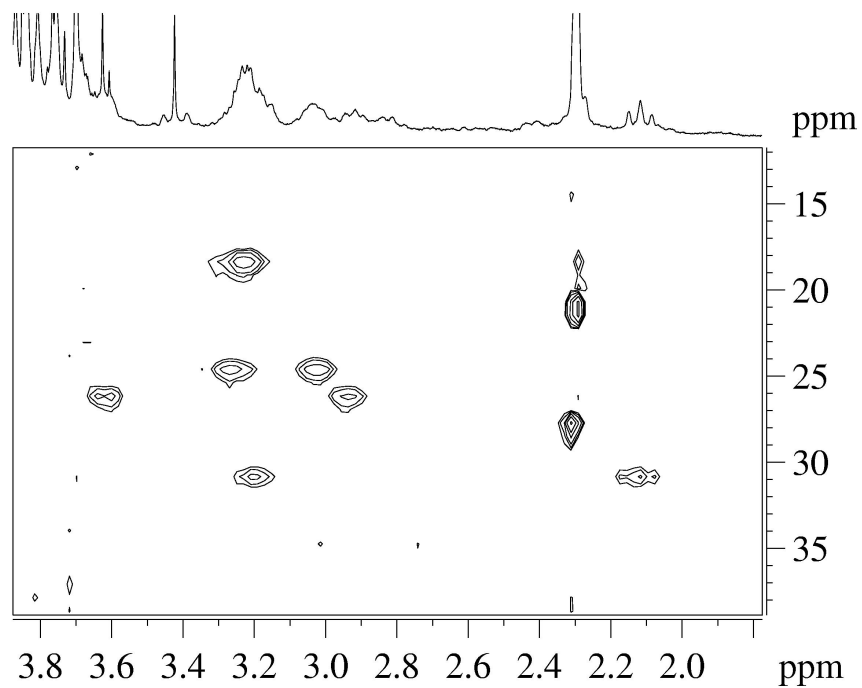


Figure S28: portion of ^1H - ^{13}C HMQC spectrum of **5** (CD_2Cl_2 , 295 K): methylene region.

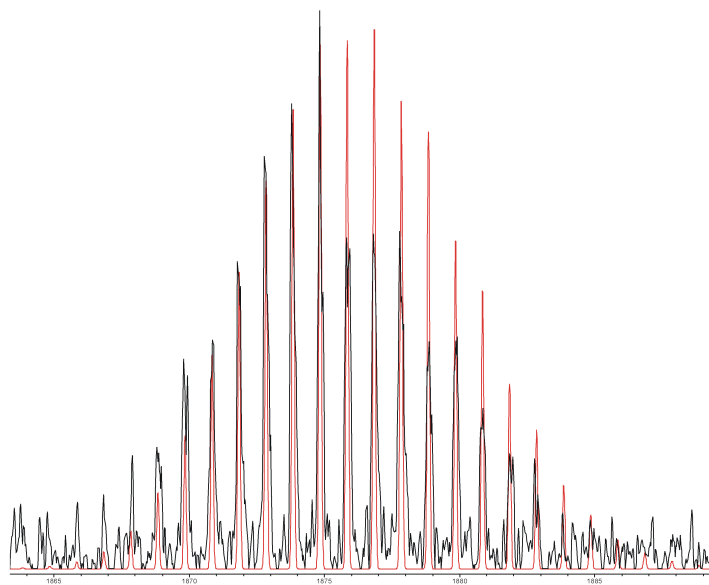
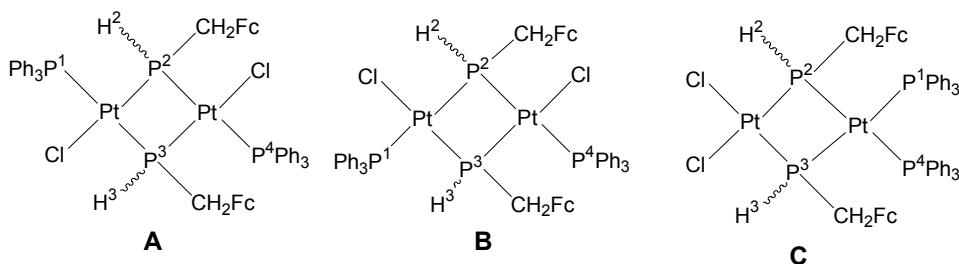
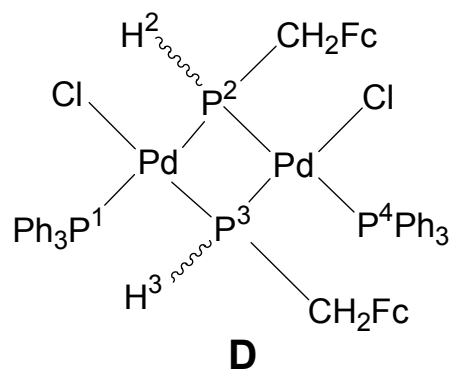


Figure S29: Experimental (black line) and simulated (red line) HRMS(+) spectrum of **5** (exact mass = 1871.8175 da) in THF diluted with CH₃CN. The error between simulated and observed isotopic patterns is 3.5 ppm.



| | P(1) | P(2) | P(3) | P(4) | H(2) | H(3) |
|-------------|---------------|-------------|-------------|-------------|-------------|-------------|
| P(1) | 22.9 | 5.0 | 385.9 | - | - | - |
| | 23.8 | 348 | - | - | - | - |
| | 23.7 | 7.9 | 382.0 | - | - | - |
| P(2) | -173.4 | 179.6 | 385.9 | 300 | - | - |
| | -181.7 | 180.0 | 348.0 | 357 | - | - |
| | -190.0 | 183.9 | 382.0 | 340 | - | - |
| P(3) | -173.4 | 5.0 | - | 300 | - | - |
| | -164.7 | - | - | 360 | - | - |
| | -190.0 | 7.9 | - | 340 | - | - |
| P(4) | 22.9 | - | - | - | - | - |
| | 23.8 | - | - | - | - | - |
| | 23.7 | - | - | - | - | - |
| H(2) | 1.51 | - | - | - | - | - |
| | 3.72 | - | - | - | - | - |
| | 2.04 | - | - | - | - | - |
| H(3) | 1.51 | - | - | - | - | - |
| | 0.05 | - | - | - | - | - |
| | 2.04 | - | - | - | - | - |

Table S1. ^{31}P and ^1H NMR parameters for complexes **A** (top), **B** (middle), and **C** (bottom), deriving from PPh_3 addition to **2**. (C_6D_6 , 295 K, 162 MHz); chemical shifts (bold) are in ppm; coupling constants (normal) are in Hz.



| | P(1) | P(2) | P(3) | P(4) | H(2) | H(3) |
|-------------|-------------|-------------|-------------|-------------|-------------|-------------|
| P(1) | 18.6 | 355 | - | - | - | - |
| P(2) | -147.7 | 245 | 355 | 355 | 355 | - |
| P(3) | | -91.6 | - | - | - | 351 |
| P(4) | | | 18.6 | - | - | - |
| H(2) | | | | 3.06 | - | - |
| H(3) | | | | | 3.70 | - |

Table S2. ^{31}P and ^1H NMR parameters for complex **D** (CD_2Cl_2 , 295 K, 162 MHz); chemical shifts (bold) are in ppm; coupling constants (normal) are in Hz.